

## Modeling core impurity reduction via divertor gas injection in NSTX

E. T. Meier<sup>1</sup>, V. A. Soukhanovskii<sup>1</sup>, R. E. Bell<sup>2</sup>, S. Gerhardt<sup>2</sup>, R. Kaita<sup>2</sup>, H. W. Kugel<sup>2</sup>, B. P. LeBlanc<sup>2</sup>, J. E. Menard<sup>2</sup>, S. F. Paul<sup>2</sup>, T. D. Rognlien<sup>1</sup>, F. Scotti<sup>2</sup>, M. V. Umansky<sup>1</sup>

<sup>1</sup> Lawrence Livermore National Laboratory, Livermore, USA

<sup>2</sup> Princeton Plasma Physics Laboratory, Princeton, USA

In the National Spherical Torus Experiment (NSTX), the use of lithium-coated graphite plasma-facing components led to improved confinement and suppression of edge localized modes (ELMs) in H-mode discharges [1, 2]. As a consequence, carbon and metal impurities tended to accumulate in the core plasma, resulting in  $Z_{eff} \leq 3 - 4$  and  $P_{rad} \leq 1 - 3$  MW. This motivated experimental efforts aimed at impurity concentration reduction in the core by, e.g., triggered ELMs [3] or impurity source reduction by divertor deuterium ( $D_2$ ) injection. This paper discusses interpretation of the latter experiment with the two-dimensional multi-fluid edge transport code, UEDGE [4, 5, 6]. A qualitative understanding of the effects of  $D_2$  injection on carbon transport behavior in the SOL is sought.

**Experiment** Two discharges from the NSTX divertor  $D_2$  injection experiment are studied: A reference shot with no divertor  $D_2$  injection, and a shot with  $D_2$  injection (gas puff). Both of these discharges were lower single-null configurations, and employed neutral beam injection (NBI) heating of 4 MW. In the shot with the gas puff, the valve of the divertor  $D_2$  injection system [7] was opened for 100 ms starting at  $t = 300$  ms. A total of approximately  $1.25 \times 10^{21}$  deuterium atoms were injected at an average injection rate of 2000 atom-amps ( $1 \text{ s}^{-1} = 1.6 \times 10^{-19} \text{ A}$ ).

Figure 1 shows the plasma performance of the two shots. The line density and stored energy were similar for shots, which were both ELM-free as evidenced by the lack of spikes in the  $D_\alpha$  light.  $Z_{eff}$  and radiated power were reduced significantly for the shot with  $D_2$  injection. Charge-exchange recombination spectroscopy (CHERS) measurements of carbon concentration measurements in the core and near the pedestal (not shown) indicate reductions of approximately 30%.

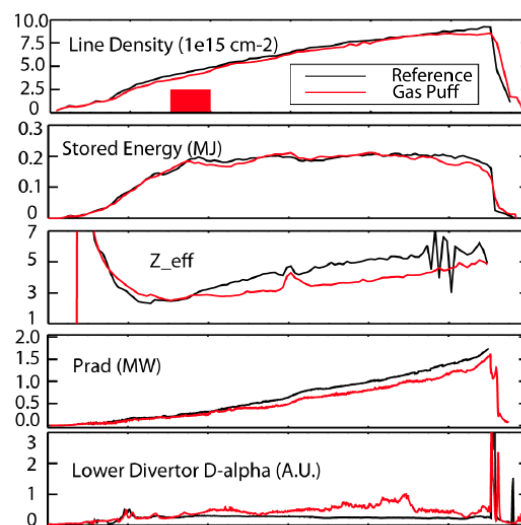


Figure 1: Key diagnostic traces for divertor deuterium gas injection experiment. The black and red curves show data for the reference shot and gas injection shot, respectively.

Lithium evaporators (LITERs) were used to apply lithium to the divertor plasma-facing components in these discharges. Experimental evidence suggests that significant carbon sputtering occurred at the outer divertor target despite the lithium coating, possibly because of nearly complete erosion of the lithium layer at the strike point.

Modeling results are compared to a variety of NSTX plasma edge diagnostics. At the outer midplane (OMP), Thomson scattering provides electron temperature and density data and CHERS measures the density and temperature of fully-stripped carbon ( $C^{6+}$ ). At the lower/outer divertor target, an infrared camera was used to measure heat flux, and filtered visible cameras measure  $D_\alpha$  and CII spectroscopic data.

**Modeling details** UEDGE is used to model the NSTX edge plasma. The effects of the divertor gas puff are studied by scanning  $D_2$  injection rates ( $I_{gas}$ ) from 0 to 1200 A. A multi-species carbon model ( $C^{1+} - C^{6+}$ ) is used. Physical and chemical sputtering are included at the divertor targets, and chemical sputtering is included at the private flux and vessel wall boundaries. The sputtering models, adapted from the DIVIMP code [8], assume uncoated graphite surfaces. The computational grid, shown in Figure 2, is based on an LRDFIT equilibrium for the reference shot at 700 ms, and captures the normalized flux range  $0.96 < \psi_N < 1.028$ . The upper X-point prevents extension of the grid to larger  $\psi_N$  without resorting to a more complicated double-null grid. Constant, uniform diffusivities are used to model anomalous perpendicular transport:  $\chi_i = \chi_e = 1.5 \text{ m}^2/\text{s}$ , and  $D_\perp = 0.5 \text{ m}^2/\text{s}$ . The inner and outer divertor target recycling coefficients are set to 0.9, simulating ion pumping by the lithium coating. Zero flux boundary conditions are applied for all carbon species and for neutral deuterium at the core-edge interface. Deuterium ion flux from the core is fixed. The core-to-edge power is 3 MW (allowing for radiation of 25% of the 4-MW NBI power). An inward pinch, simulating the convective (blob) transport [10], is applied to the carbon ion species such that the impurity concentration at  $\psi_N = 0.96$  is approximately 5% ( $v_{pinch} = -25 \text{ m/s}$ ). Drift effects are not included.

Steady-state UEDGE solutions are compared to experimental data at  $t \approx 700 \text{ ms}$ . Experimental outer midplane (OMP) temperature and density profiles for shots with and without divertor gas puff are qualitatively similar. For all scanned values of  $I_{gas}$ , UEDGE  $T_e$

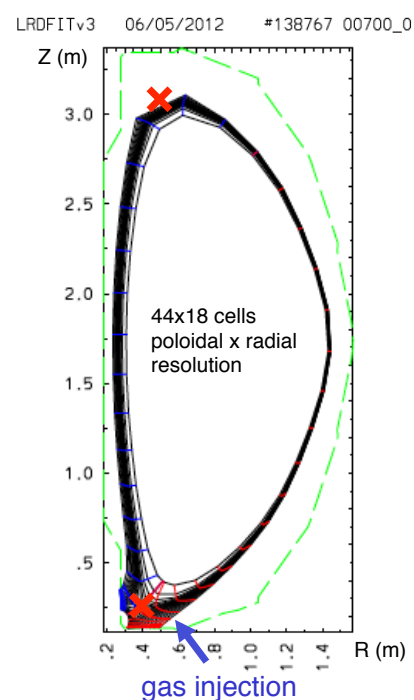


Figure 2: The computational grid for UEDGE modeling. Red X's indicate X-point locations.

**Results and discussion** Steady-state UEDGE solutions are compared to experimental data at  $t \approx 700 \text{ ms}$ . Experimental outer midplane (OMP) temperature and density profiles for shots with and without divertor gas puff are qualitatively similar. For all scanned values of  $I_{gas}$ , UEDGE  $T_e$

profiles are similar to experimental profiles, which are shifted such that the Thomson  $T_e$  matches the UEDGE  $T_e$  at the OMP separatrix ( $\approx 75$  eV). OMP separatrix electron density is near  $3 \times 10^{19} \text{ m}^{-3}$  in UEDGE vs.  $1.5 \times 10^{19} \text{ m}^{-3}$  in the experiment, but notably, the UEDGE OMP separatrix density rises with increasing  $I_{gas}$  reaching, e.g.,  $4.5 \times 10^{19}$  at 1000 A.  $D_\alpha$  profiles on the outer divertor target are in good agreement, with UEDGE intensity agreeing at  $I_{gas} = 0$  A and 1000 A with experimentally measured intensities for the reference and gas puff shots, respectively, to within 15%. UEDGE CII (658 nm) profiles for  $I_{gas} = 0$  A and 1000 A have peak intensities 2-3 times higher than the experimental values for the reference and gas puff shots, respectively. Peak heat flux for the UEDGE 0 A case is  $\approx 6 \text{ MW/m}^2$ , whereas the experimental peak heat flux for the reference shot is  $\approx 2.5 \text{ MW/m}^2$ . For the UEDGE 1000 A case, the peak heat flux is reduced to  $\approx 2 \text{ MW/m}^2$ , which is similar to the peak heat flux for the shot with divertor gas puff.

The primary results of the UEDGE modeling are presented in Figure 3. As the deuterium injection rate increases, the carbon concentration at the outer midplane separatrix generally decreases, with 40% reduction at  $I_{gas}=1000$  A. Sputtered flux is generated predominantly at the divertor targets. With  $I_{gas}=0$  A, sputtered flux from the outer divertor target is composed of 99 A chemical sputtering and 64 A physical sputtering. With increasing gas injection, the divertor temperatures drop, and physical sputtering is reduced to practically zero. Chemical sputtering increases, roughly compensating the reduction of physical sputtering.

Figure 4 reveals underlying physics that may play a role in the carbon concentration reduction. The top

panel shows total carbon density plotted along a field line from the outer midplane (OMP) to the outer divertor target on the 2 mm flux surface. In the bottom panel, deuterium ion and average carbon ion flow speeds are shown along the same field line. With no gas injection, the carbon ion flow is away from the target along most of the field line, but stagnates near the OMP. In contrast, with 1000 A gas injection, the flow out of the divertor continues past the OMP without stagnation. This carbon transport modification is probably driven by the dramatic change in the deuterium flow: instead of flowing strictly from the OMP to the target, the deuterium flow has

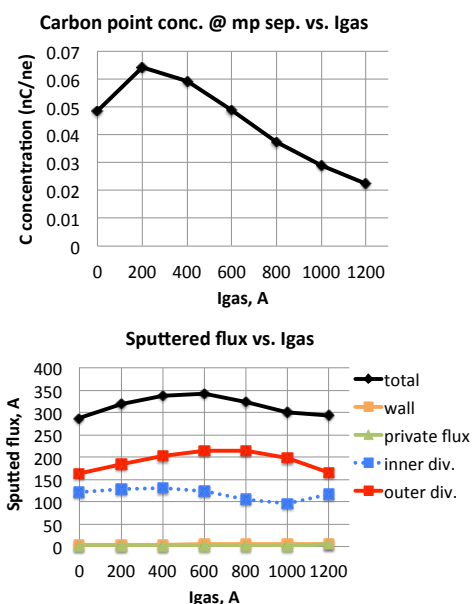


Figure 3: Top and bottom panels show carbon concentration at the outer midplane separatrix, and sputtered flux, respectively, plotted as functions of simulated gas injection rate.

reversed, now flowing toward the OMP from a location significantly below the X-point. In general, impurity parallel flow is strongly influenced by the friction force between the deuterium and impurity flows (which is primarily balanced by the ion temperature gradient force) [11]. Reversal of the deuterium flow thus facilitates the reversal of the carbon flow. The resulting carbon "flow-through" past the OMP seems related to the reduction of peak carbon concentration.

**Conclusions** These UEDGE results provide indications of the physical mechanisms behind carbon concentration reduction via divertor gas injection in NSTX. The reversal of the deuterium flow at the outer midplane SOL seems to entrain and prevent stagnation of the carbon flow, reducing carbon concentration despite an essentially constant sputtered carbon influx. These results form the basis for continued analysis in future work. In future work, possible modeling improvements include: grid extensions both deeper into the core and closer to the outer vessel wall; an improved sputtering model (perhaps accounting for lithium effects); more closely matched midplane profiles (perhaps by using radially variable transport coefficients).

**Acknowledgements** This work was performed under U.S. Department of Energy Contracts DE-AC52-07NA27344 and DE AC02-09CH11466.

## References

- [1] M. G. Bell et al. *Plasma Phys. Control. Fusion*, 51:124054, 2009.
- [2] R. Maingi et al. *Phys. Rev. Lett.*, 103:075001, 2009.
- [3] J. M. Canik et al. *Phys. Rev. Lett.*, 104:045001, 2010.
- [4] T. D. Rognlien, J. L. Milovich, M. E. Rensink, and G. D. Porter. *J. Nucl. Mater.*, 196:347 – 351, 1992.
- [5] T. D. Rognlien and D. D. Ryutov. *Plasma Phys. Rep.*, 25:943–957, 1999.
- [6] T. D. Rognlien and M. E. Rensink. *Fusion Eng. Design*, 60:497 – 514, 2002.
- [7] V. A. Soukhanovskii et al. *Nucl. Fusion*, 49:095025, 2009.
- [8] P. C. Stangeby and J. D. Elder. *Nucl. Fusion*, 35:1391–1412, 1995.
- [9] C. Hopf, W. Jacob, et al. *J. Nucl. Mater.*, 342:141–147, 2005.
- [10] A. Yu. Pigarov et al. *Contrib. Plasma Phys.*, 44:228–234, 2004.
- [11] P. C. Stangeby. Taylor & Francis Group, 2000.

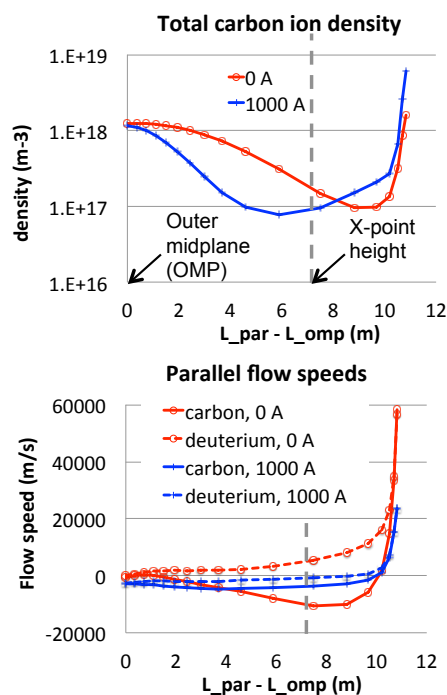


Figure 4: Carbon ion density and carbon and deuterium parallel flow speeds as a function of distance along a field line from the outer midplane to the outer divertor target on the 2-mm flux surface.